



LJMU Research Online

Köhnke, MC, Siekmann, I, Seno, H and Malchow, H

A type IV functional response with different shapes in a predator-prey model.

<http://researchonline.ljmu.ac.uk/id/eprint/13486/>

Article

Citation (please note it is advisable to refer to the publisher's version if you intend to cite from this work)

Köhnke, MC, Siekmann, I, Seno, H and Malchow, H (2020) A type IV functional response with different shapes in a predator-prey model. Journal of Theoretical Biology, 505. ISSN 0022-5193

LJMU has developed **LJMU Research Online** for users to access the research output of the University more effectively. Copyright © and Moral Rights for the papers on this site are retained by the individual authors and/or other copyright owners. Users may download and/or print one copy of any article(s) in LJMU Research Online to facilitate their private study or for non-commercial research. You may not engage in further distribution of the material or use it for any profit-making activities or any commercial gain.

The version presented here may differ from the published version or from the version of the record. Please see the repository URL above for details on accessing the published version and note that access may require a subscription.

For more information please contact researchonline@ljmu.ac.uk

A type IV functional response with different shapes in a predator-prey model

Merlin C. Köhnke^{a,*}, Ivo Siekmann^b, Hiromi Seno^c, Horst Malchow^a

^a*Institute of Mathematics, School of Mathematics/Computer Science, Osnabrück University, Germany*

^b*Liverpool John Moores University, Department of Applied Mathematics, Liverpool, L3 3AF, England*

^c*Research Center for Pure and Applied Mathematics, Graduate School of Information Sciences, Tohoku University, Aramaki-Aza-Aoba 6-3-09, Aoba-ku, Sendai, 980-8579, Japan*

Abstract

Group defense is a phenomenon that occurs in many predator-prey systems. Different functional responses with substantially different properties representing such a mechanism exist. Here, we develop a functional response using timescale separation. A prey-dependent catch rate represents the group defense. The resulting functional response contains a single parameter that controls whether the group defense functional response is saturating or dome-shaped. Based on that, we show that the catch rate must not increase monotonically with increasing prey density to lead to a dome-shaped functional response. We apply bifurcation analysis to show that non-monotonic group defense is usually more successful. However, we also find parameter regions in which a paradox occurs. In this case, higher group defense can give rise to a stable limit cycle, while for lower values, the predator would go extinct. The study does not only provide valuable insight on how to include functional responses representing group defense in mathematical models, but it also clarifies under which circumstances the usage of different functional responses is appropriate.

Keywords: type IV functional response, dome-shaped functional response, group defense

*Corresponding author

Email address: merlin.koehnke@uos.de (Merlin C. Köhnke)

¹ 1. Introduction

² Predation is a ubiquitous interaction in ecological communities (Allan,
³ 1995). The dynamics of mathematical models describing predator-prey rela-
⁴ tionships depend critically on the functional response (Abrams and Ginzburg,
⁵ 2000; Gross et al., 2004; Aldebert et al., 2016). The most commonly used
⁶ functional responses rely on the work of Holling (1959) and Holling (1961).
⁷ These are categorized as Holling type I, II, and III functional responses. How-
⁸ ever, a wide range of other functional responses exist as well, and even though
⁹ the shape of the functional response is similar (for instance, the Holling type
¹⁰ II and the Ivlev functional response (Ivlev, 1961)), the dynamics may change
¹¹ qualitatively (Aldebert et al., 2016). This phenomenon is called structural
¹² sensitivity.

¹³ In this study, we will focus on a mathematical predator-prey model incor-
¹⁴ porating a group defense of the prey. It is well known that some prey species
¹⁵ adapt to predation and can develop different avoidance or defense strategies
¹⁶ (Jeschke, 2006). Some bacteria, for instance, produce toxins that may be
¹⁷ lethal for eukaryotic predators (Lainhart et al., 2009). However, avoidance
¹⁸ strategies such as flight, freezing (Blanchard et al., 1986), using refuge ar-
¹⁹ eas, or a combination of these (Blanchard et al., 1990) usually do not have
²⁰ a direct negative impact on the predator population (Edmunds, 1974). In-
²¹ stead, decreasing the attack success due to predator confusion can reduce the
²² predation without harming the predator (Allee, 1958; Jeschke and Tollrian,
²³ 2005). For instance, moose use intimidation of wolves as a non-harmful de-
²⁴ fense strategy (Caro, 2005). Another example is given by plankton sensing
²⁵ predator kairomones leading to morphological changes, which is a success-
²⁶ ful defense strategy against size-selective predators (Lass and Spaak, 2003).
²⁷ Besides, many species warn conspecifics of the group using alarm signals
²⁸ (Klump and Shalter, 1984). Such a swarming effect often occurs in social
²⁹ populations (Tener, 1965; Líznarová and Pekár, 2013).

³⁰ In mathematical models, anti-predator defense strategies have often been
³¹ incorporated by a potentially adaptive decrease in handling time, an increase
³² in attack rates, or a combination of these two (Jeschke and Tollrian, 2000;
³³ Líznarová and Pekár, 2013; Köhnke, 2019). However, as many of the de-
³⁴ fense mechanisms depend on the population size of the prey (Krams et al.,
³⁵ 2009), often also a dome-shaped functional response is used. The charac-

teristic feature of a dome-shaped functional response is that the consumed
 prey for a particular prey density has a maximum at finite prey densities.
 Different experiments have confirmed the dome-shape, such as Pekár (2005),
 as well as Líznarová and Pekár (2013). However, group defense is likely to be
 present in many systems, although not indicated by the functional response
 (Jeschke and Tollrian, 2005). Even though, not in his classical paper about
 functional responses (Holling (1959)), in 1961, already Holling has proposed
 four functional responses, one of them incorporating a swarming effect leading
 to a dome-shaped functional response. Hence, this is often referred to
 as a Holling type IV functional response (Huang and Xiao, 2004; Lian and
 Xu, 2009; Wang et al., 2009). However, classically only type I, II, and III are
 referred to as Holling types. To avoid confusion, we will stick to the term
 type IV functional response throughout this paper.

Different expressions exist for such a type IV functional response (Tostowaryk, 1972; Fujii et al., 1986; Líznarová and Pekár, 2013). Particularly
 some studies use a type IV functional response with a square prey dependence
 in the denominator but without any linear dependence (Zhang et al.,
 2006; Baek, 2010). These usually have a form similar to

$$f_{IV}(U) = \frac{U}{1 + U^2}. \quad (1)$$

This form was originally proposed by Sokol and Howell (1981) as a simplification of a functional response that also incorporates a linear prey dependence in the denominator. Such kind of response is sometimes referred to as Monod-Haldane functional response (Andrews, 1968) and is commonly used as well (Edwards, 1970; Chen, 2004; Upadhyay and Raw, 2011). Collings (1997) derived a similar functional response resulting from the assumption that searching efficacy and handling time are decreasing and increasing with prey density, respectively.

In section 2, we develop a functional response based on a quasi-steady-state assumption. Applying quasi-steady-state assumptions is a powerful tool ranging back to Bodenstein (1913). It can help to significantly simplify dynamical systems using the idea that processes described by the dynamical system happen on different timescales (Shoffner and Schnell, 2017). We will show that, if the catch rate is monotonically increasing with prey density, the resulting functional response will be saturating. Otherwise, the functional response can be dome-shaped. We will analyze the rather general model analytically before we introduce a functional response incorporating a group

72 defense in section 3. The shape of this functional response can be varied
 73 using a single parameter. We will treat this model analytically and with
 74 bifurcation analysis to show that the group defense can drive the predator
 75 to extinction. However, we will also show that for a small parameter region,
 76 a paradox occurs.

77 2. General model

78 We start with developing a predator-prey model of the form

$$79 \quad \frac{dU}{dT} = \Phi(U) - f(U)V, \quad U(0) = U_0, \quad (2a)$$

$$80 \quad \frac{dV}{dT} = Q(f(U)V) - mV, \quad V(0) = V_0 \quad (2b)$$

81 with

$$82 \quad \Phi(0) = \Phi(K) = 0, \quad \Phi'(K) < 0. \quad (2c)$$

84 with all parameters being positive. Here, K represents the carrying capacity
 85 of the prey population. The prey U grows according to the function $\Phi(U)$ in
 86 absence of the predator V . This function has at least two stationary states,
 87 the extinction, and the carrying capacity. Furthermore, the carrying capacity
 88 is stable in absence of the predator. We model the mortality of the predator
 89 with a linear term. The term $f(U)$ is the functional response, i.e., how the
 90 number of predicated prey per unit time of one average predator varies with
 91 changing densities. Note that we are interested in group defense and thus
 92 assume that the functional response is only affected by the prey density. The
 93 function $Q(f(U)V)$ represents the biomass production of V due to predation,
 94 i.e., the numerical response.

95 To develop the functional response, we assume that the predator can be
 96 divided into two separate states, searching and handling, i.e., $V = S + H$.
 97 Note that an alternative approach to develop a functional response is by
 98 argumentations on time budgets of the prey. An example regarding group
 99 behavior is given by Braza (2012). The dynamics of the subpopulations are
 100 given by

$$101 \quad \frac{dS}{dT} = -\beta g(U)S + \gamma H, \quad S(0) = S_0, \quad g(0) = 0, \quad (3a)$$

$$102 \quad \frac{dH}{dT} = \beta g(U)S - \gamma H, \quad H(0) = H_0. \quad (3b)$$

104 This approach also allows for the derivation of a Holling type II functional
 105 response (Diekmann et al., 2012). Note that we neglect birth and death
 106 processes here, assuming that they happen on a much slower timescale (for
 107 a discussion on the validity of such a timescale separation see Appendix A).
 108 Hence, $V = S + H = \text{const.}$ holds for this timescale. Searching individuals
 109 turn into handling individuals by capturing prey with a rate β depending
 110 on the function $g(U)$. The function $g(U)$ represents the rate of successful
 111 catch and kill per searching predator, while β represents the search rate.
 112 Throughout the manuscript, we will refer to $g(U)$ as *catch rate*. Note that
 113 in this interpretation, handling individuals are all individuals that are not
 114 actively searching for prey, for instance, handling prey or digesting it. After
 115 some handling time $\tau = \gamma^{-1}$, handling individuals turn back into searching
 116 individuals.

117 Applying time-scale separation, we can find a quasi-stationary solution
 118 for the searching subpopulation

$$S^* = \frac{\gamma V}{\beta g(U) + \gamma}. \quad (4)$$

119 Now, we assume that predation depends only on searching individuals which
 120 allows us to introduce the functional response

$$f(U)V = \beta g(U)S^* = \gamma V \frac{\beta g(U)}{\beta g(U) + \gamma}. \quad (5)$$

121 For monotonically increasing catch rates, the resulting functional response
 122 will also increase monotonically. Hence, dome-shaped functional responses
 123 only occur if the catch rate is not monotonically increasing.

124 To derive the functional response in this way and not to incorporate it di-
 125 rectly into the model has three advantages. First, it may be easier to measure
 126 in some cases as the predation process is split up into two separate processes,
 127 i.e., searching and handling. For the conversion of searching into handling
 128 individuals, it is sufficient to introduce an entirely searching (not satiated)
 129 predator population into a prey population of different sizes to retrieve the
 130 catch rate depending on the prey population. For many experiments, that is
 131 the case anyway. However, note that one must be cautious with such mea-
 132 surements as a discrepancy between local measurements and a mean-field
 133 functional response, e.g., over a heterogeneous vertical water column, may
 134 exist (Morozov and Arashkevich, 2008; Morozov, 2010). Furthermore, only

135 the time between searching events needs to be measured. Second, it shows
 136 under which assumptions a type IV functional response of the form given by
 137 Eq. (1) emerges, which will show the artificiality of this form. Third and
 138 most important for this study, it allows us to introduce a single parameter
 139 later on that changes the functional response from a saturating form into a
 140 dome-shaped form to differentiate the effect of different group defense forms
 141 from other factors.

142 For simplicity, we assume that the numerical response depends linearly
 143 on the functional response (for a discussion on alternatives see Abrams and
 144 Ginzburg (2000)). In particular, this means that conversion of prey biomass
 145 into predator biomass is proportional to the predation term with a propor-
 146 tionality constant e , which one can interpret as conversion efficiency. Assum-
 147 ing that the timescale separation is valid, this yields

$$148 \quad \frac{dU}{dT} = \Phi(U) - \beta \frac{\gamma g(U)V}{\beta g(U) + \gamma}, U(0) = U_0, \quad (6a)$$

$$149 \quad \frac{dV}{dT} = e\beta \frac{\gamma g(U)V}{\beta g(U) + \gamma} - mV, V(0) = V_0 \quad (6b)$$

151 for the original predator-prey model. Note that this form is similar to
 152 a functional response in Jeschke et al. (2002), incorporating a probability
 153 of a predator searching for prey in the classical Holling type II functional
 154 response.

155 This model has two stationary solutions, that always exist, i.e.,

$$156 \quad E_0 = (U_0^*, V_0^*) = (0, 0), \quad (7a)$$

$$157 \quad E_c = (U_c^*, V_0^*) = (K, 0). \quad (7b)$$

159 Depending on the growth dynamics $\Phi(U)$, more semi-trivial solutions may
 160 exist. Furthermore, depending on the form of the function $g(U)$, non-trivial
 161 solutions E_n^* may exist. These take the form

$$162 \quad g(U_n^*) = \frac{m\gamma}{\beta(e\gamma - m)}, \quad (8a)$$

$$163 \quad 164 \quad V_n^* = \frac{e\Phi(U_n^*)}{m}. \quad (8b)$$

165 Hence, the predator can only survive in coexistence with its prey. The
 166 function $g(U)$ is by definition a catch rate and, thus, $g(U_n^*) \geq 0$. For the

167 existence of these solutions, this yields

$$\text{e}\gamma > m, \quad (9\text{a})$$

$$\Phi(U_n^*) > 0. \quad (9\text{b})$$

171 From a biological perspective, this means that the conversion efficiency e and
172 the handling rate γ , which are both related to predation abilities, need to be
173 larger than the mortality of the predator. As we assume that handling prey
174 takes place on a shorter timescale than birth and death processes, Eq. (9a)
175 likely holds. Interestingly, a higher value of the searching rate β cannot
176 compensate for lower handling rates regarding the existence of the coexistence
177 solution.

178 For the linear stability of the stationary solutions, we consider the Jaco-
179 bian

$$J = \begin{pmatrix} \Phi'(U) - \frac{\beta\gamma^2 g'(U)V}{(\gamma + \beta g(U))^2} & -\frac{\beta\gamma g(U)}{\gamma + \beta g(U)} \\ \frac{e\beta\gamma^2 V g'(U)}{(\gamma + \beta g(U))^2} & \frac{e\beta\gamma g(U)}{\gamma + \beta g(U)} - m \end{pmatrix}. \quad (10)$$

180 Evaluation at the trivial solution E_0 yields the eigenvalues $\lambda_{0,1} = \Phi'(0)$ and
181 $\lambda_{0,2} = -m$. Hence, the trivial solution is always a saddle in absence of a
182 strong Allee effect and a stable node in presence of a strong Allee effect.

183 The Jacobian evaluated at the semi-trivial solution E_c has the eigenval-
184 ues $\lambda_{c,1} = \Phi'(K)$, and $\lambda_{c,2} = \frac{\beta g(K)(e\gamma - m) - \gamma m}{\gamma + \beta g(K)}$. Hence, if no coexistence
185 solutions exist, i.e., $e\gamma \leq m$, the semi-trivial solution is a stable node. Con-
186 versely, if coexistence is possible,

$$g(K) < \frac{m\gamma}{\beta(e\gamma - m)} = g(U_n^*). \quad (11)$$

187 must hold as a stability criterion. If $g(U)$ is monotonically increasing in U ,
188 this can never hold as $K > U_n^*$. However, for a non-monotonic predation
189 rate, the carrying capacity may be stable if a coexistence solution exists.
190 Hence, bistability between coexistence and carrying capacity may occur.

191 We address the stability of the coexistence solution(s) using the Routh-
192 Hurwitz-criterion. After some simplification involving particularly Eqs. 8,
193 one gets

$$\text{Tr}(J|_{E_n^*}) = \Phi'(U_n^*) - \kappa g'(U_n^*)\Phi(U_n^*) < 0 \quad (12\text{a})$$

$$\det(J|_{E_n^*}) = \frac{\kappa g'(U_n^*)\Phi(U_n^*)}{m} > 0 \quad (12\text{b})$$

¹⁹⁷ with $\kappa = \frac{\beta(m - e\gamma)^2}{e\gamma^2 m}$ as conditions for stability of the coexistence solution(s). If the coexistence solution(s) exist(s), only

$$g'(U_n^*) > 0 \quad (13)$$

¹⁹⁹ must hold for a positive determinant. Note that this is assured for a monotonically increasing catch rate. If this holds, Eq. (12a) can be rewritten as

$$\frac{\Phi'(U_n^*)}{g'(U_n^*)\Phi(U_n^*)} < \kappa. \quad (14)$$

²⁰¹ Hence, if the conditions before hold, a sufficient condition for stability is that $\Phi'(U_n^*) < 0$. Clearly, if the coexistence state is unstable but existent in case ²⁰³ of a monotonically increasing functional response, an asymptotically stable ²⁰⁴ periodic solution must exist as the only possible stable attractor. If Eq. (13) ²⁰⁵ and $Tr(J|_{E_n^*}) = 0$ hold, a Hopf bifurcation occurs (Britton, 2012). As $J_{2,2} = 0$ ²⁰⁶ at the coexistence solution, the second condition requires $J_{1,1} = 0$, i.e., the ²⁰⁷ bifurcation occurs at the maximum of the nontrivial prey nullcline.

²⁰⁸ From a biological perspective, the stability criterion given by Eq. (14) ²⁰⁹ means that the growth function of the prey needs to be sufficiently high, i.e., ²¹⁰ $\Phi(U_n^*) \gg 0$. Furthermore, the change of the catch rate with increasing prey ²¹¹ densities $g'(U_n^*)$ needs to be sufficiently large. To visualize this relationship, ²¹² Fig. 1 shows different growth functions of the prey and different functional ²¹³ responses emerging from given catch rates. The figure shows five general ²¹⁴ tendencies. First, logistic growth tends to stabilize coexistence compared to ²¹⁵ a strong Allee effect (upper panel). Second, as $g'(U_n^*) > 0$ for monotonically ²¹⁶ increasing functions, the coexistence equilibrium is always stable if it exists ²¹⁷ in the dark blue regions for these functional responses. Third, the light blue ²¹⁸ line corresponds to the often used type IV functional response, cf. Eq. (1). ²¹⁹ As its derivative with respect to the prey is particularly high at low den- ²²⁰sities, it tends to overestimate the stability of the coexistence equilibrium ²²¹ at these densities compared to other functional responses representing group ²²² defense (red and green curve). Fourth, group defense with critical population ²²³ size, i.e., a dome-shaped functional response, is more successful at high prey ²²⁴ densities as it makes the stability of the coexistence equilibrium unlikely. ²²⁵ Conversely, group defense leading to a saturation (green curve) is more suc- ²²⁶cessful for equilibria at low prey densities. Fifth, if the prey population obeys ²²⁷ a strong Allee effect with a higher Allee threshold than the threshold of the ²²⁸ group defense, coexistence can never be stable.

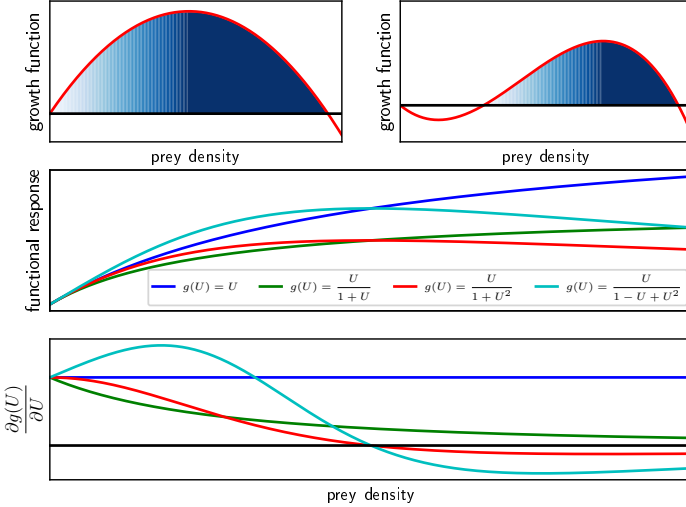


Figure 1: **A type IV functional response as in Eq. (1) overestimates stability of coexistence solutions at low prey densities.** The upper panel shows logistic growth and growth with a strong Allee effect. For stability, Eqs. (12) need to hold. If $g'(U_n^*)$, shown in the lower panel, is negative, stable coexistence is not possible. If it is positive, stability is guaranteed in the dark blue regions in the upper panel. Otherwise, coexistence becomes more likely with higher $\Phi(U_n^*)$ as indicated by the blue shade and higher $g'(U_n^*)$. The panel in the middle shows the value of different functional responses $f(U)$ (ordinate) depending on the prey density. The colors indicate the underlying catch rates $g(U)$.

229 3. Model with a given catch rate

230 Depending on the catch rate, the resulting functional response could rep-
 231 resent diverse biological phenomena, such as saturation, e.g., $g(U) = U$ or
 232 prey switching, e.g., $g(U) = U^2$. Here, we want to investigate the potential
 233 impact of group defense. Group defense can be represented by the catch rate

$$g(U) = \frac{U}{1 + (\frac{U}{C})^\nu}. \quad (15)$$

234 The form of this function is arbitrary to a certain extent. However, we will see
 235 that the shape of the functional response changes by varying ν from satura-
 236 tion to different dome-shaped functional responses. Most studies assume an
 237 exponent $\nu \geq 1$. However, some studies also indicate $\nu < 1$ for species with

herding behavior such as group defense (Braza, 2012). If $\nu > 1$, a dome-shaped functional response emerges while if $\nu \leq 1$, a saturating functional response emerges. If $C \gg K$, the resulting functional response coincides with the Holling type II functional response. However, if the critical value is $C < K$, it controls the impact of a higher prey density if $\nu \leq 1$. In case of $\nu > 1$, it represents a critical value beyond which the group defense has a high impact. In the following, we will refer to it as the *critical defense value*.

The derivative of this function at low densities is given by

$$\lim_{U \rightarrow 0} g'(U) = 1. \quad (16)$$

Hence, the rate of change at low densities is not affected by this function, but it impacts the shape of the curve at higher densities.

In particular,

$$\lim_{U \rightarrow \infty} g'(U) = 0 \quad (17)$$

holds at high densities. For $\nu \leq 1$, this leads to saturation of the catch rate like in the Holling type II functional response, whereas for $\nu > 1$, the catch rate has a maximum at

$$U_{max} = C(\nu - 1)^{-\frac{1}{\nu}} \quad (18)$$

meaning that higher prey densities lead to lower predation success. Even with $\nu > 1$, the model can represent different dome-shaped functional responses such as one with a linear and quadratic term (Líznarová and Pekár, 2013) or with a linear and cubic term (Tostowaryk, 1972) in the denominator.

Incorporating this function in the general model, i.e., Eq. (6), yields

$$\frac{dU}{dT} = \Phi(U) - V \frac{\beta\gamma U}{\gamma + \beta U + \gamma(U/C)^\nu}, \quad (19a)$$

$$\frac{dV}{dT} = eV \frac{\beta\gamma U}{\gamma + \beta U + \gamma(U/C)^\nu} - mV. \quad (19b)$$

It can be seen that the linear term can be neglected as in Eq. (1) only if the search rate of the predator β and handling time γ^{-1} are sufficiently small and/or if $C \ll K$. In this case, the nonlinear term in the denominator is the leading term.

Regarding the stability of the carrying capacity, we already know that it is stable if no coexistence solution exists. Otherwise, $e\gamma > m$ holds and given the functional response above

$$\frac{K}{1 + (\frac{K}{C})^\nu} < g(U_n^*) \quad (20)$$

267 needs to hold for stability. This demonstrates that low critical defense values
 268 and high group defense strengths increase the likelihood that the carrying
 269 capacity is stable.

270 Regarding the number of coexistence solutions, we can simplify Eq. (8a)
 271 to

$$U_n^{*\nu} = \frac{C^\nu}{g(U_n^*)} U_n^* - C^\nu. \quad (21)$$

272 Hence, a necessary condition for the existence of a coexistence solution is
 273 $U_n^* > g(U_n^*)$. Depending on ν , the potential number of stationary coexistence
 274 solutions differ. Only in the non-monotonic case, i.e., $\nu > 1$, more than one
 275 coexistence solution can exist.

276 In particular, if $\nu < 1$, $U_n^{*\nu}$ is a concave function. As the right hand side
 277 of Eq. (21) is a straight line intersecting the abscissa at $U = g(U_n^*) > 0$, one
 278 intersection always exists. If $\nu = 1$, the left-hand side and the right-hand
 279 side intersect at

$$U_n^* = \frac{Cg(U_n^*)}{C - g(U_n^*)}. \quad (22)$$

280 Hence, $C > g(U_n^*)$ needs to hold for the existence of a coexistence solution.
 281 Furthermore, $\Phi(U_n^*) > 0$ must hold for feasibility.

282 If $\nu > 1$, $U_n^{*\nu}$ is a convex function. Hence, either zero or two solutions
 283 exist for almost all parameter combinations satisfying $\Phi(U_n^*) > 0$. However,
 284 note that $\Phi(U_n^*) > 0$ may also just hold for one of the nontrivial solutions. In
 285 this case, the other vertical predator nullcline is at positive densities but is
 286 not biologically meaningful as it is beyond the carrying capacity. Rewriting
 287 Eq. (21) yields

$$\phi(U_n^*) = U_n^{*\nu} - \frac{C^\nu}{g(U_n^*)} U_n^{*\nu} + C^\nu = 0. \quad (23)$$

288 As this function has a minimum at the positive value

$$U_{n\min}^* = \sqrt[\nu-1]{\frac{C^\nu}{\nu g(U_n^*)}} \quad (24)$$

289 and $\phi(0) = C^\nu > 0$, $\phi(U_{n\min}^*) < 0$ must hold for the feasibility of two
 290 coexistence solutions. This corresponds to

$$g(U_n^*) < g(U_n^*)_{crit} = \frac{(\nu-1)(C^{-\nu}(\nu-1))^{-\frac{1}{\nu}}}{\nu}. \quad (25)$$

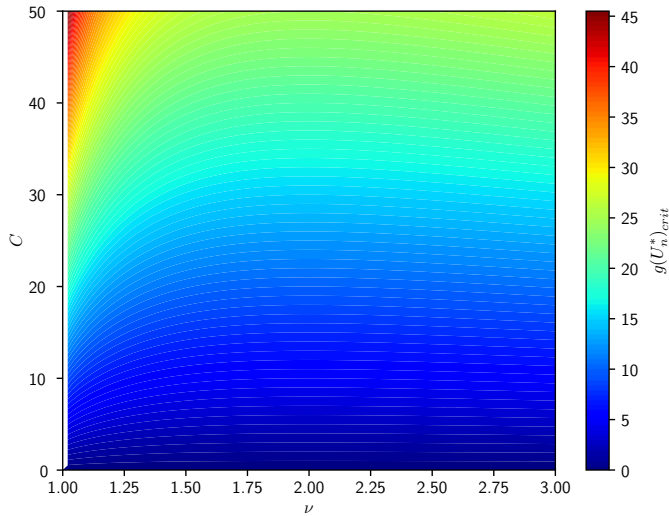


Figure 2: **The likelihood of the feasibility of a second coexistence solution tends to increase with a higher critical defense value and higher group defense strength.** The threshold $g(U_n^*)_{crit}$ given by Eq. (25) is visualized. Low values denoted by blue colors correspond to situations in which the feasibility of two coexistence solutions is unlikely. Note that for $\nu \leq 1$, two coexistence solutions are never possible.

At $g(U_n^*) = g(U_n^*)_{crit}$, a saddle-node bifurcation takes place. The threshold $g(U_n^*)_{crit}$ is visualized in Fig. 2. The color scale shows the maximum value of $g(U_n^*)$ for feasibility of two coexistence solutions. For higher values of C , the critical value of $g(U_n^*)$ increases monotonically. Hence, a higher critical defense value makes the feasibility of two coexistence solutions more likely. This relationship becomes more complex regarding the strength of the group defense. The function $g(U_n^*)(C, \nu)$ shows a minimum at $\nu = 2$. This corresponds to the classical function of group defense, which thus may tend to underestimate the existence of two coexistence solutions. However, note that this effect is very weak.

Now, we consider the stability of the coexistence solutions. By Eqs. (13) and (12a), we know that

$$g'(U_n^*) = \frac{C^\nu(C^\nu - (\nu - 1)U_n^{*\nu})}{(C^\nu + U_n^{*\nu})^2} \quad (26)$$

303 is a crucial expression for the stability of the nontrivial equilibrium. In
 304 particular, a necessary condition for stability is $g'(U_n^*) > 0$, which always
 305 holds if $\nu \leq 1$. However, if a maximum of the catch rate exists at finite
 306 population densities, i.e., $\nu > 1$,

$$U_n^* < \eta(\nu) = \sqrt[\nu]{\frac{C^\nu}{\nu - 1}} \quad (27)$$

307 must hold for stability. Note that this corresponds to the maximum of the
 308 catch rate given by Eq. (18), meaning that in case of group defense, stable
 309 coexistence is only possible at prey densities smaller than the prey density
 310 at the maximum of the catch rate. Note that this is already visualized in
 311 Fig. 1. From this condition, we can see (Appendix B) that

$$\lim_{\nu \rightarrow \infty} \eta(\nu) = C \quad (28)$$

312 and

$$\lim_{\nu \rightarrow 1^+} \eta(\nu) = \infty. \quad (29)$$

313 Furthermore, for $\nu = 2$, $\eta(\nu) = C$ holds. Hence, for high group defense
 314 values as well as for $\nu = 2$, prey and predator can only coexist at values
 315 $U_n^* < C$ underlining the criticality of this parameter. There is no biologically
 316 meaningful threshold close to saturation of the catch rate. Note that this is
 317 only a necessary condition for stability. As a sufficient condition, $g'(U)$ needs
 318 to be sufficiently large. It is obvious that

$$g''(U_n^*) = -\frac{\nu C^\nu U_n^{*\nu-1} ((1+\nu)C^\nu - (\nu-1)U_n^{*\nu})}{(C^\nu + U_n^{*\nu})^3} \quad (30)$$

319 is negative if $\nu \leq 1$. Furthermore, if $\nu > 1$, $g''(U_n^*)$ is negative if

$$U_n^{*\nu} < \frac{(1+\nu)C^\nu}{\nu-1}. \quad (31)$$

320 As

$$\frac{C^\nu}{\nu-1} < \frac{(1+\nu)C^\nu}{\nu-1}, \quad (32)$$

321 one can say from Eq. (27) that $g'(U_n^*)$ is a monotonically decreasing function
 322 in U_n^* as long as $g'(U_n^*)$ is positive. Thus, with smaller values of U_n^* , stability of
 323 the equilibrium gets more likely. However, in these regions, stable coexistence

324 is unlikely due to the growth functions (see Fig. 1). In particular, if a strong
 325 Allee effect is present, this makes coexistence unlikely as $\Phi(U_n^*) > 0$ needs to
 326 hold as well. Hence, a strong Allee effect prevents stable coexistence at low
 327 densities while group defense prevents stable coexistence at high densities.
 328 Thus, a combination of a strong Allee effect in the prey and group defense
 329 may be detrimental for predators.

Tab. 1 summarizes the feasibility and stability conditions of model (19).

Table 1: Feasibility and stability of solutions for model (19) assuming that $\Phi(U) = 0$ only at $U = 0$ and $U = K$, i.e., in absence of a strong Allee effect.

Solution	Feasibility	Stability
$(U_0, V_0) = (0, 0)$	unconditionally feasible	unconditionally unstable
$(U_c, V_0) = (K, 0)$	unconditionally feasible	if $e\gamma \leq m$ or if $g(K) < g(U_n^*)$
$(U_{n,1}, V_{n,1})$	nec.: $U_n^* > g(U_n^*)$	nec.: if $\nu \leq 1$ or if $\nu > 1 \wedge U_{n,1} < \sqrt[\nu]{\frac{C^\nu}{\nu - 1}}$
$(U_{n,2}, V_{n,2})$	$\nu > 1 \wedge g(U_n^*) < g(U_n^*)_{crit}(C, \nu) \wedge \Phi(U_n^*) > 0$	nec.: $U_{n,2} < \sqrt[\nu]{\frac{C^\nu}{\nu - 1}}$

330
 331 For the numerical investigation of the model, we have chosen a logistic
 332 growth function

$$\Phi(U) = rU - cU^2 \quad (33)$$

333 where rc^{-1} represents the carrying capacity K . Fig. 3 shows a bifurcation
 334 diagram for the two parameters representing the group defense. For the
 335 remaining parameters, we used estimations based on an ecological micro-
 336 tine rodent mustelid model from Huisman and De Boer (1997) and Hanski
 337 and Korpimäki (1995) satisfying the conditions for timescale separation, see
 338 Appendix A. The usage of this case study makes sense as rodents show anti-
 339 predator behavior such as ultrasonic vocalizations as an alarm signal that
 340 can be interpreted as group defense (Blanchard et al., 1990).

341 C is the critical defense value, while ν shapes the form of the functional
 342 response. Recall that for high C , the functional response tends to the Holling
 343 type II functional response. Hence, it is evident, that group defense is bene-
 344 ficial for the prey as it increases the likelihood that the carrying capacity is
 345 the only stable stationary solution.

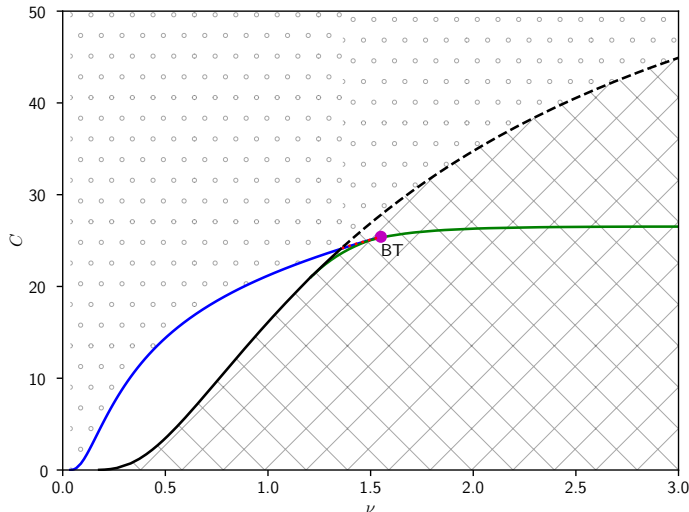


Figure 3: **Group defense can lead to extinction of the predator.** A two-dimensional bifurcation diagram with ν , and the critical defense value C as bifurcation parameters is shown. In the squared region, the prey exists at its capacity. The solid black line corresponds to a transcritical bifurcation leading to a stable coexistence state (white region). This stable coexistence state loses stability via a Hopf bifurcation (blue line), resulting in a stable limit cycle (dotted area). For higher ν , the limit cycle is destroyed via a homoclinic bifurcation that takes place simultaneously with a transcritical bifurcation (dashed black line). Note that between green, blue, and black solid lines, the system is bistable. It depends on the initial conditions, whether the system converges to the stable coexistence state or the carrying capacity of the prey. BT indicates the Bogdanov-Takens bifurcation point. From this point, a homoclinic bifurcation (red dotted line) emerges. Below this line, a small parameter region corresponding to bistability between a limit cycle and the carrying capacity exists. The remaining parameters are as stated in Appendix A. We computed the bifurcation curves using XPPAUT (Ermentrout, 2002).

346 At higher values of ν or low values of C , the carrying capacity of the
 347 prey is the only stable stationary solution. Hence, it is evident that stronger
 348 group defense is beneficial for the prey population for most parameter regions.
 349 Note that the exact values of ν and C depend on the parameter set. The
 350 values stated in the following are just for reference regarding Fig. 3. For
 351 $\nu \lesssim 1.4$, a stable coexistence solution emerges for high values of C via a
 352 transcritical (solid black line) bifurcation. Increasing the value of C even

353 further, this equilibrium undergoes a Hopf bifurcation (blue line), leading
354 to a limit cycle. For $\nu \gtrsim 1.4$, this limit cycle vanishes via a homoclinic
355 bifurcation (dashed line) for sufficiently low C . This homoclinic bifurcation
356 coincides with a transcritical bifurcation. Fig. C.7 illustrates the homoclinic
357 orbit. Furthermore, for $\nu > 1$, i.e., if group defense is dome-shaped, a saddle-
358 node bifurcation exists (green line). However, note that we have only plotted
359 the saddle-node bifurcation in the parameter regions in which it takes place
360 at biologically meaningful densities. Furthermore, note that the green line
361 corresponds to a particular isocline of Fig. 2. Hence, it has a maximum value
362 $\nu = 2$.

363 Note that bifurcations have been extensively studied for predator-prey
364 models with Holling type II functional response as well as with type IV
365 functional response. However, this bifurcation diagram allows seeing the
366 impact of defense directly. In particular, if C is sufficiently low, i.e., $C \lesssim 16.1$,
367 a saturating group defense functional response is sufficient. In this case, the
368 carrying capacity is the only stable solution already at $\nu = 1$ corresponding
369 to a saturating functional response. For values higher than this threshold,
370 group defense makes leading to a non-monotonic functional response makes
371 sense as it may turn the carrying capacity into a stable equilibrium via a
372 transcritical bifurcation. However, at high values of C , corresponding to high
373 critical defense values, the transcritical bifurcation curve (and the homoclinic
374 bifurcation curve) tends to saturate. In this case, group defense does not
375 change the system dynamics. As already stated above, for very large values
376 of C , the functional response converges to the Holling type II functional
377 response. Hence, from the bifurcation diagram, it is evident that group
378 defense, in general (independent of the exact form), has the potential to
379 drive the predator to extinction.

380 On the left-hand side of the Bogdanov-Takens bifurcation, bistability can
381 occur. As the parameter regions corresponding to bistability are very small,
382 Fig. 4 shows a sketch of this region. It demonstrates that above the saddle-
383 node bifurcation, bistability can occur either with one stationary coexistence
384 state and the carrying capacity or with a stable limit cycle and the carry-
385 ing capacity. This is a phenomenon that only occurs for a non-monotonic
386 functional response. Hence, catch rates with a critical value increase the
387 complexity of the model. Furthermore, in a small parameter region, a para-
388 dox can occur. On the left-hand side and above of the red dotted homoclinic
389 bifurcation curve, the capacity is the only stable stationary solution. Increasing
390 the strength of collective defense by increasing ν or decreasing the critical

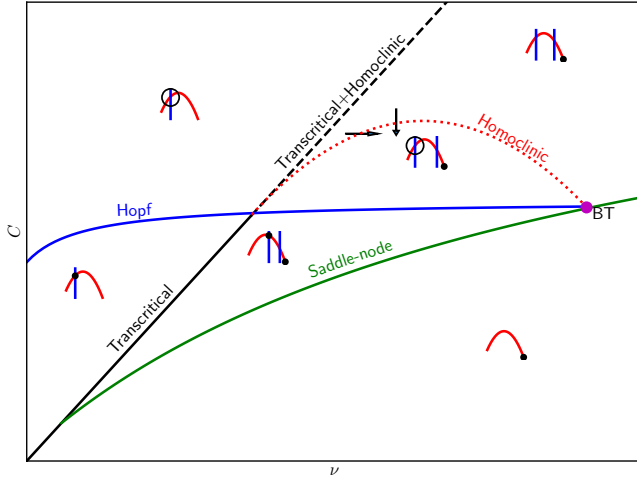


Figure 4: **In case of a non-monotonic functional response, group defense can lead to complex dynamics including a paradox.** A sketch of the region around the Bogdanov-Takens bifurcation in Fig. 3 is shown. The small plots represent sketches of the phase plane. Circles denote stable limit cycles; the black dots represent stable equilibria. Note that for convenience, we did not show the trivial nullclines. The paradox is visualized by the arrows. Here, increasing the group defense by increasing ν or decreasing C can prevent the predator from extinction.

value C , the system becomes bistable. In this case, a stable limit cycle or a stable stationary coexistence state exists. Fig. 5 shows such a transition as an illustration of this paradox. At low critical defense values, the system is bistable in this case. Starting in the region separated by the stable manifold, the system converges to a limit cycle. Increasing the value of C which can be interpreted as decreasing the collective defense efficacy leads to an increase in the amplitude of the predator-prey oscillations. At some point the limit cycle vanishes via a homoclinic bifurcation. The homoclinic orbit is shown in the middle panel. Without the stable limit cycle, the system is monostable and every initial condition converges to the prey carrying capacity. Hence, increasing the critical defense value is beneficial for the prey in this case. The same can happen with an increase of the defense strength ν .

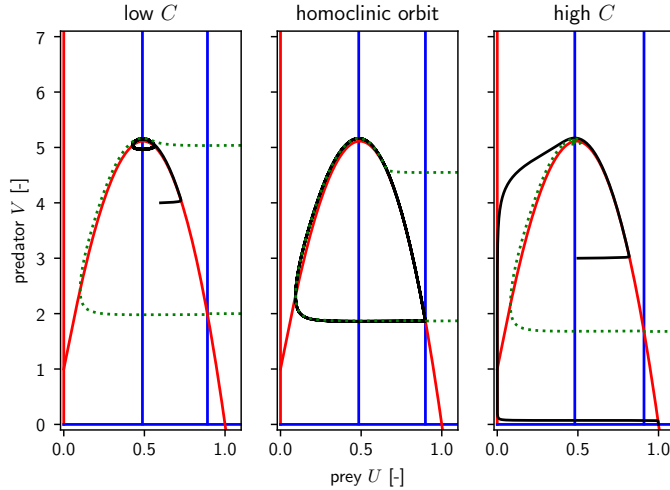


Figure 5: **Increasing the critical defense value can drive the predator to extinction.** The phase plane for three different parameter combinations are shown to illustrate the paradox. Black lines are sample trajectories, blue and red lines represent predator and prey nullclines, respectively. The dotted green lines represents the stable manifold of the saddle (right coexistence state). Parameters are $\nu = 1.38$, $C_{low} = 24.3$, $C_{homoclinic} \approx 24.32$, $C_{high} = 24.35$. The remaining parameters are as stated in Appendix A.

403 4. Discussion and Conclusion

404 In this study, we proposed a functional response incorporating group de-
 405 fense based on timescale separation arguments. Here, a dome-shape may or
 406 may not emerge. In particular, if the catch rate increases monotonously with
 407 increasing prey density, the resulting functional response is also a saturating
 408 function, although it incorporates group defense. However, compared to the
 409 Holling type II functional response, the saturation value is lower. We pro-
 410 vided an example for that, cf. green curve in Fig. 1. Group defense that
 411 is not leading to a dome-shaped functional response is commonly found in
 412 experiments (Jeschke and Tollrian, 2005; Olson et al., 2013). Thus, with
 413 our approach, we obtain a class of group defense functional responses that
 414 can represent at least two biologically meaningful shapes. Hence, with the
 415 derivation, we also underpin the idea that group defense is likely to be present
 416 in many systems, although not clearly indicated by the measured functional
 417 response (Jeschke and Tollrian, 2005).

418 The dome-shaped functional response emerges only if a critical prey den-
419 sity exists beyond which the catch rate decreases again, cf. the red curve in
420 the lower panel of Fig 1. This is a valuable finding as the mechanisms lead-
421 ing to dome-shaped functional responses are not fully understood for some
422 systems (Mezzalira et al., 2017).

423 From a modeling perspective, we have shown that the type IV functional
424 response, as in Eq. (1), potentially overestimates stable coexistence at low
425 prey densities. If the prey population exists at low densities, the type IV
426 functional response without linear prey dependence in the denominator seems
427 to be a good approximation. However, we have shown that the linear term
428 in the denominator is only negligibly small if the searching rate and the
429 handling time are low and/or the critical defense value is much lower than
430 the carrying capacity of the prey. This is a strong assumption for many
431 predator-prey relationships. Indeed, some ecological studies even lead to the
432 conclusion that the linear component in the denominator in the functional
433 response is much more pronounced than the quadratic component (Líznarová
434 and Pekár, 2013). If this is not clear, a functional response, as proposed in
435 this study, should preferably be used.

436 For a saturating functional response, only one nontrivial equilibrium can
437 exist, while for a dome-shaped functional response, up to two coexistence
438 equilibria can occur. This allows for the possibility of a homoclinic bifurca-
439 tion in the model and increases the complexity of the behavior in general.
440 Regarding the stability of coexistence, a strong Allee effect in the prey com-
441 bined with a dome-shaped functional response shrinks the interval of the prey
442 density in which stable coexistence is possible. Furthermore, we have applied
443 bifurcation analysis for the defense parameters showing that group defense
444 increases the extinction probability of the predator. However, for low critical
445 defense values, a saturating functional response is sufficient as the carrying
446 capacity of the prey is the only stable attractor. The same holds for very high
447 critical defense values. In this case, group defense does not have a qualitative
448 impact and should thus be omitted if it is related to costs.

449 Finally, we have shown that for a small range of parameters, a paradox
450 can occur. Lowering the critical defense value or increasing the strength
451 of the group defense gives rise to stable coexistence (either stationary or
452 oscillatory) that is not possible at slightly higher critical defense value or
453 lower strength of the group defense. However, it needs further investigations
454 to know whether this paradox can occur over larger parameter regimes and
455 thus would have ecological relevance.

456 **Appendix A. Timescale separation**

457 One necessary assumption for the validity of the timescale separation
 458 is that birth and death processes happen on another timescale compared
 459 to other processes such as predation or competition. In particular, following
 460 Segel (1988), we can find a characteristic timescale for the processes described
 461 by Eq. (3). Assuming that changes in U and V are sufficiently small compared
 462 to changes in S and H , we set $U = U_0$ and $V = V_0$ and rewrite Eq. (3a)
 463 yielding

$$\frac{dS}{dt} = -(\beta g(U_0) + \gamma) \left(S - \frac{\gamma V_0}{\beta g(U_0) + \gamma} \right). \quad (\text{A.1})$$

464 In this form, the stationary solution, as well as the characteristic timescale
 465 $t_S = l^{-1} = (\gamma + \beta g(U_0))^{-1}$ is directly visible. If l is large compared to the
 466 vital parameters of the populations, U and V do not change significantly in
 467 this time, and the timescale separation is valid. In particular, this approach
 468 illustrates that the parameters β and γ need to be large compared to the
 469 magnitude of $\Phi(U)$ and m representing birth and death processes.

470 More specifically, this holds if the upper bound of the flow per character-
 471 istic time interval is significantly small. An approximation for this is given
 472 by

$$\max \left(\left| t_S \frac{dU}{dT} \right|_{max}, \left| t_S \frac{dV}{dT} \right|_{max} \right) \ll \Upsilon. \quad (\text{A.2})$$

473 Here, Υ depends on the order of magnitude of the state variables. Note that
 474 this is just an estimation as the flow may be changing in the time interval
 475 $[t, t + t_S]$. However, as the flow depends continuously on the state variables
 476 and the time interval is small, this estimate will give a reasonable value.

477 To investigate whether the timescale separation is valid, we use a logistic
 478 growth function and parameterize the model with the same two parameter
 479 sets as in Huisman and De Boer (1997). In particular, they use one parameter
 480 set from Scheffer and De Boer (1995) corresponding to an algae zooplankton
 481 model and one parameter set from Hanski and Korpimäki (1995) correspond-
 482 ing to a microtine rodent mustelid model. As our functional response looks
 483 slightly different from the classical Holling type II functional response, we
 484 estimate the parameters β and γ with a Gradient method, see, e.g., Polak
 485 (2012).

486 The adjusted parameters for the algae zooplankton model are $r = 0.5$
 487 day^{-1} , $c = 0.05 \text{ l (day mg DW)}^{-1}$, $e = 0.6$, $\beta = 0.67 \text{ l (day mg DW)}^{-1}$,
 488 $\gamma = 0.4 \text{ day}^{-1}$, $m = 0.15 \text{ day}^{-1}$. If either the equation for the prey or the

489 predator changes significantly, the timescale separation approach is not valid.
 490 For convenience, we let $V \rightarrow 0$ and examine only $|\Phi(U)t_S|$ depending on the
 491 exact form of $g(U)$. This is a biologically relevant parameter choice as it may
 492 correspond to a predator invading into a habitat with only prey. Fig. A.6 a)
 shows the dependence on the density of the prey and on ν . It can be seen that

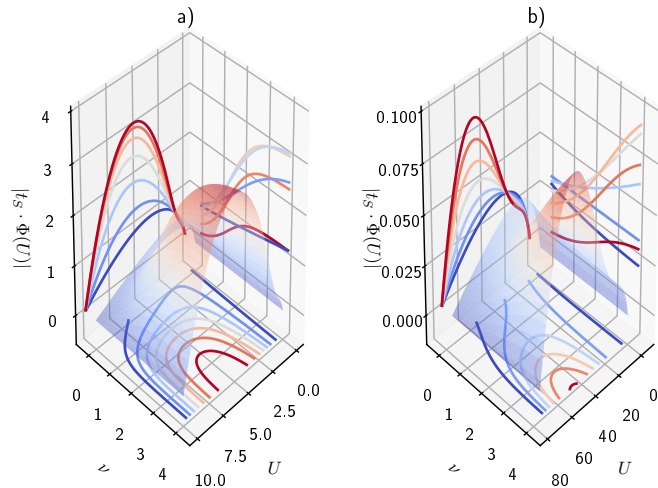


Figure A.6: **For the algae zooplankton model, the timescale separation is not valid while it is valid for the rodent mustelid model.** The expression $z = |\Phi(U)t_S|$ is plotted for different defense strengths ν and different population sizes of the prey U . The right panel refers to the rodent mustelid model. In this case, the steady-state assumption is valid based on this expression, while it is not valid for the zooplankton model (left panel). Furthermore, it can be seen (contours in the $U, z - plane$) that stronger group defense make the validity of the quasi-steady-state assumption less likely while it seems to be most likely for low or high prey densities.

493
 494 the quasi-steady-state assumption does not hold for this parameter set for
 495 most values of U . Furthermore, higher values of ν tend to increase the length
 496 of the time interval and thus make the quasi-steady-state assumption even
 497 worse. Note that a reason for the failure of the timescale separation may
 498 be the short lifespan of microorganisms. This becomes directly apparent,
 499 comparing the intrinsic death rate m with the predation parameters β and
 500 γ .

501 The adjusted parameters for the rodent mustelid model are $r = 4.05$
 502 year^{-1} , $c = 0.054 \text{ ha (individuals year)}^{-1}$, $e = 0.0023$, $\beta = 118.7 \text{ ha (individuals year)}^{-1}$,
 503 $\gamma = 600.7 \text{ year}^{-1}$, $m = 1 \text{ year}^{-1}$. In this case, the rate of
 504 change of the growth function is comparably low (Fig. A.6 b)). Note that
 505 in the predation terms, the validity does not only depend on one species but
 506 on both species. However, for relevant combinations of U and V , i.e., com-
 507 binations with densities that are realistic in the phase plane, the timescale
 508 separation still holds in this case As before, higher values of ν tend to increase
 509 the rate of change. However, for the predation term, this only holds until a
 510 maximum of $\nu \approx 2$. Beyond this threshold, the function is decreasing again.
 511 Nevertheless, in models without group defense, the validity of the timescale
 512 separation seems to be more likely.

513 Appendix B. Limit of $\eta(\nu)$

$$\begin{aligned}
 \lim_{\nu \rightarrow \infty} \sqrt[\nu]{\frac{C^\nu}{\nu - 1}} &= \lim_{\nu \rightarrow \infty} \exp \ln \sqrt[\nu]{\frac{C^\nu}{\nu - 1}} \\
 &= \lim_{\nu \rightarrow \infty} \exp \frac{\ln \frac{C^\nu}{\nu - 1}}{\nu} \\
 &= \exp \lim_{\nu \rightarrow \infty} \frac{\ln C^\nu - \ln (\nu - 1)}{\nu}
 \end{aligned}$$

514 The numerator grows asymptotically slower than ν , thus $\lim_{\nu \rightarrow \infty} -\frac{\ln (\nu - 1)}{\nu} =$
 515 0. Furthermore, as $\ln C^\nu / \nu = \nu \ln C / \nu = \ln C$, $\lim_{\nu \rightarrow \infty} \sqrt[\nu]{\frac{C^\nu}{\nu - 1}} = C$ holds.

516 Appendix C. Homoclinic orbit

517 Fig. C.7 illustrates a sample trajectory close to the homoclinic orbit that
 518 coincides with the transcritical bifurcation. At the transcritical bifurcation,
 519 the right predator nullcline gives rise to a second coexistence equilibrium.

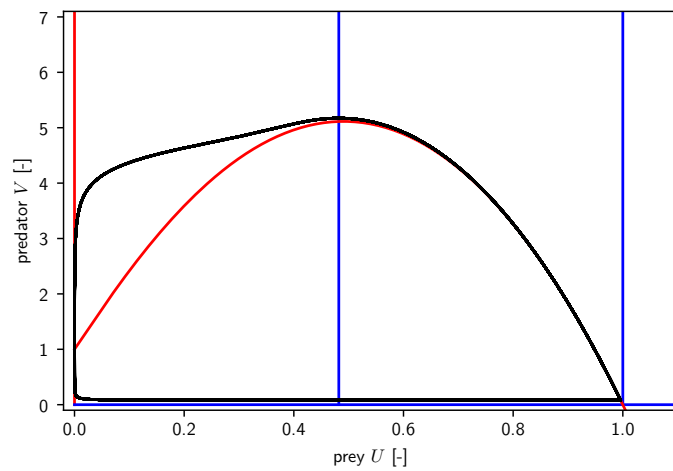


Figure C.7: The homoclinic orbit destroying the limit cycle in the monostable case coincides with a transcritical bifurcation. The phase plane for three different parameter combinations are shown to illustrate the paradox. The black line is a sample trajectory close to the homoclinic orbit, blue and red lines represent predator and prey nullclines, respectively. Parameters are $\nu = 1.36$ and $C = 24.2$. The remaining parameters are as stated in Appendix A.

520 **Acknowledgments**

521 The Japan Society for the Promotion of Science (JSPS) that provided
522 funding for a stay at Tohoku University for MCK and HM supported this
523 work. MCK acknowledge discussions with Frank M. Hilker about the bifur-
524 cation analysis.

- 525 Abrams, P. A. and Ginzburg, L. R. (2000). The nature of predation: prey
526 dependent, ratio dependent or neither? *Trends in Ecology & Evolution*,
527 15(8):337–341.
- 528 Aldebert, C., Nerini, D., Gauduchon, M., and Poggiale, J. (2016). Structural
529 sensitivity and resilience in a predator–prey model with density-dependent
530 mortality. *Ecological Complexity*, 28:163–173.
- 531 Allan, J. D. (1995). Predation and its consequences. In *Stream Ecology*,
532 pages 163–185. Springer.
- 533 Allee, W. (1958). The social life of animals, revised edn.
- 534 Andrews, J. F. (1968). A mathematical model for the continuous culture
535 of microorganisms utilizing inhibitory substrates. *Biotechnology and Bio-*
536 *engineering*, 10(6):707–723.
- 537 Baek, H. (2010). A food chain system with Holling type IV functional re-
538 sponse and impulsive perturbations. *Computers & Mathematics with Ap-*
539 *plications*, 60(5):1152–1163.
- 540 Blanchard, R. J., Blanchard, D. C., Rodgers, J., and Weiss, S. M. (1990).
541 The characterization and modelling of antipredator defensive behavior.
542 *Neuroscience & Biobehavioral Reviews*, 14(4):463–472.
- 543 Blanchard, R. J., Flannelly, K. J., and Blanchard, D. C. (1986). Defensive be-
544 haviors of laboratory and wild *Rattus norvegicus*. *Journal of Comparative*
545 *Psychology*, 100(2):101.
- 546 Bodenstein, M. (1913). Eine Theorie der photochemischen Reaktsions-
547 geschwindigkeiten. *Zeitschrift für physikalische Chemie*, 85(1):329–397.
- 548 Braza, P. A. (2012). Predatorprey dynamics with square root functional
549 responses. *Nonlinear Analysis: Real World Applications*, 13(4):1837–1843.
- 550 Britton, N. F. (2012). *Essential mathematical biology*. Springer Science &
551 Business Media.
- 552 Caro, T. (2005). *Antipredator defenses in birds and mammals*. University of
553 Chicago Press.

- 554 Chen, Y. (2004). Multiple periodic solutions of delayed predator–prey sys-
555 tems with type IV functional responses. *Nonlinear Analysis: Real World*
556 *Applications*, 5(1):45–53.
- 557 Collings, J. B. (1997). The effects of the functional response on the bifur-
558 cation behavior of a mite predator–prey interaction model. *Journal of*
559 *Mathematical Biology*, 36(2):149–168.
- 560 Diekmann, O., Heesterbeek, H., and Britton, T. (2012). *Mathematical tools*
561 *for understanding infectious disease dynamics*, volume 7. Princeton Uni-
562 versity Press.
- 563 Edmunds, M. (1974). *Defence in animals: a survey of anti-predator defences*.
564 Longman Publishing Group.
- 565 Edwards, V. H. (1970). The influence of high substrate concentrations on
566 microbial kinetics. *Biotechnology and Bioengineering*, 12(5):679–712.
- 567 Ermentrout, B. (2002). *Simulating, analyzing, and animating dynamical sys-*
568 *tems: a guide to XPPAUT for researchers and students*, volume 14. Siam.
- 569 Fujii, K., Holling, C., and Mace, P. (1986). A simple generalized model of
570 attack by predators and parasites. *Ecological research*, 1(2):141–156.
- 571 Gross, T., Ebenhöh, W., and Feudel, U. (2004). Enrichment and foodchain
572 stability: the impact of different forms of predator–prey interaction. *Jour-*
573 *nal of theoretical biology*, 227(3):349–358.
- 574 Hanski, I. and Korpimäki, E. (1995). Microtine rodent dynamics in northern
575 Europe: parameterized models for the predator-prey interaction. *Ecology*,
576 76(3):840–850.
- 577 Holling, C. (1961). Principles of insect predation. *Annual review of entomol-*
578 *ogy*, 6(1):163–182.
- 579 Holling, C. S. (1959). The components of predation as revealed by a study
580 of small-mammal predation of the European pine sawfly. *The Canadian*
581 *Entomologist*, 91(5):293–320.
- 582 Huang, J.-C. and Xiao, D.-M. (2004). Analyses of bifurcations and stability
583 in a predator-prey system with Holling type-IV functional response. *Acta*
584 *Mathematicae Applicatae Sinica*, 20(1):167–178.

- 585 Huisman, G. and De Boer, R. J. (1997). A formal derivation of the Beddington functional response. *Journal of theoretical biology*, 185(3):389–400.
- 586
- 587 Ivlev, V. S. (1961). *Experimental ecology of the feeding of fishes*. Yale University Press, New Haven.
- 588
- 589 Jeschke, J. M. (2006). Density-dependent effects of prey defenses and predator offenses. *Journal of theoretical biology*, 242(4):900–907.
- 590
- 591 Jeschke, J. M., Kopp, M., and Tollrian, R. (2002). Predator functional responses: discriminating between handling and digesting prey. *Ecological Monographs*, 72(1):95–112.
- 592
- 593
- 594 Jeschke, J. M. and Tollrian, R. (2000). Density-dependent effects of prey defences. *Oecologia*, 123(3):391–396.
- 595
- 596 Jeschke, J. M. and Tollrian, R. (2005). Effects of predator confusion on functional responses. *Oikos*, 111(3):547–555.
- 597
- 598 Klump, G. and Shalter, M. (1984). Acoustic behaviour of birds and mammals in the predator context; I. Factors affecting the structure of alarm signals. II. The functional significance and evolution of alarm signals. *Zeitschrift für Tierpsychologie*, 66(3):189–226.
- 599
- 600
- 601
- 602 Köhnke, M. (2019). Invasion dynamics in an intraguild predation system with predator-induced defense. *Bulletin of mathematical biology*, 81(10):3754–3777.
- 603
- 604
- 605 Krams, I., Bērziņš, A., and Krama, T. (2009). Group effect in nest defence behaviour of breeding pied flycatchers, *Ficedula hypoleuca*. *Animal Behaviour*, 77(2):513–517.
- 606
- 607
- 608 Lainhart, W., Stolfa, G., and Koudelka, G. B. (2009). Shiga toxin as a bacterial defense against a eukaryotic predator, *Tetrahymena thermophila*. *Journal of bacteriology*, 191(16):5116–5122.
- 609
- 610
- 611 Lass, S. and Spaak, P. (2003). Chemically induced anti-predator defences in plankton: a review. *Hydrobiologia*, 491(1-3):221–239.
- 612
- 613 Lian, F. and Xu, Y. (2009). Hopf bifurcation analysis of a predator-prey system with Holling type IV functional response and time delay. *Applied Mathematics and Computation*, 215(4):1484–1495.
- 614
- 615

- 616 Líznarová, E. and Pekár, S. (2013). Dangerous prey is associated with a type
617 4 functional response in spiders. *Animal behaviour*, 85(6):1183–1190.
- 618 Mezzalira, J. C., Bonnet, O. J., Carvalho, P. C. d. F., Fonseca, L., Bremm,
619 C., Mezzalira, C. C., and Laca, E. A. (2017). Mechanisms and implications
620 of a type IV functional response for short-term intake rate of dry matter in
621 large mammalian herbivores. *Journal of Animal Ecology*, 86(5):1159–1168.
- 622 Morozov, A. and Arashkevich, E. (2008). Patterns of zooplankton functional
623 response in communities with vertical heterogeneity: a model study. *Math-
624 ematical Modelling of Natural Phenomena*, 3(3):131–148.
- 625 Morozov, A. Y. (2010). Emergence of Holling type III zooplankton functional
626 response: bringing together field evidence and mathematical modelling.
627 *Journal of theoretical biology*, 265(1):45–54.
- 628 Olson, R. S., Hintze, A., Dyer, F. C., Knoester, D. B., and Adami, C. (2013).
629 Predator confusion is sufficient to evolve swarming behaviour. *Journal of
630 The Royal Society Interface*, 10(85):20130305.
- 631 Pekár, S. (2005). Predatory characteristics of ant-eating Zodarion spiders
632 (Araneae: Zodariidae): potential biological control agents. *Biological Con-
633 trol*, 34(2):196–203.
- 634 Polak, E. (2012). *Optimization: algorithms and consistent approximations*,
635 volume 124. Springer Science & Business Media.
- 636 Scheffer, M. and De Boer, R. J. (1995). Implications of spatial heterogeneity
637 for the paradox of enrichment. *Ecology*, 76(7):2270–2277.
- 638 Segel, L. A. (1988). On the validity of the steady state assumption of enzyme
639 kinetics. *Bulletin of mathematical biology*, 50(6):579–593.
- 640 Shoffner, S. and Schnell, S. (2017). Approaches for the estimation of
641 timescales in nonlinear dynamical systems: Timescale separation in en-
642 zyme kinetics as a case study. *Mathematical biosciences*, 287:122–129.
- 643 Sokol, W. and Howell, J. (1981). Kinetics of phenol oxidation by washed
644 cells. *Biotechnology and Bioengineering*, 23(9):2039–2049.
- 645 Tener, J. (1965). Muskoxen. *Queens Printer, Ottawa*.

- 646 Tostowaryk, W. (1972). The effect of prey defense on the functional re-
647 sponse of *Podisus modestus* (Hemiptera: Pentatomidae) to densities of
648 the sawflies *Neodiprion swainei* and *N. pratti banksiana* (Hymenoptera:
649 Neodiprionidae). *The Canadian Entomologist*, 104(1):61–69.
- 650 Upadhyay, R. K. and Raw, S. N. (2011). Complex dynamics of a three species
651 food-chain model with Holling type IV functional response. *Nonlinear
652 Anal. Model. Control*, 16(3):353–374.
- 653 Wang, Q., Dai, B., and Chen, Y. (2009). Multiple periodic solutions of an
654 impulsive predator-prey model with Holling-type IV functional response.
655 *Mathematical and Computer Modelling*, 49(9-10):1829–1836.
- 656 Zhang, S., Tan, D., and Chen, L. (2006). Chaos in periodically forced Holling
657 type II predator-prey system with impulsive perturbations. *Chaos, Soli-
658 tons & Fractals*, 28(2):367–376.